

Spatial Reuse in IEEE 802.11bn Coordinated Multi-AP WLANs: A Throughput Analysis

David Nunez^b, Francesc Wilhelmi^{*}, Lorenzo Galati-Giordano^{*},
Giovanni Geraci^{#b}, and Boris Bellalta^b

^b*Department of Information and Communications Technologies, Universitat Pompeu Fabra, Barcelona, Spain*

^{*}*Radio Systems Research, Nokia Bell Labs, Stuttgart, Germany*

[#]*Telefónica Research, Barcelona, Spain*

Abstract—IEEE 802.11 networks continuously adapt to meet the stringent requirements of emerging applications like cloud gaming, eXtended Reality (XR), and video streaming services, which require high throughput, low latency, and high reliability. To address these challenges, Coordinated Spatial Reuse (C-SR) can potentially contribute to optimizing spectrum resource utilization. This mechanism is expected to enable a higher number of simultaneous transmissions, thereby boosting spectral efficiency in dense environments and increasing the overall network performance. In this paper, we focus on the performance analysis of C-SR in Wi-Fi 8 networks. In particular, we consider an implementation of C-SR where channel access and inter-Access Point (AP) communication are performed over the air using the Distributed Coordination Function (DCF). For such a purpose, we leverage the well-known Bianchi's throughput model and extend it to support multi-AP transmissions via C-SR. Numerical results in a WLAN network that consists of four APs show C-SR throughput gains ranging from 73% to 284% depending on the inter-AP distance and the position of the stations in the area.

Index Terms—Coordinated Spatial Reuse, IEEE 802.11bn, Multi-Access Point Coordination, Wi-Fi 8.

I. INTRODUCTION

Next-generation applications such as eXtended Reality (XR), high-quality holographic video, and zero-delay file exchange to support cooperative and remote working require further improvements on wireless networks [1]. For example, the throughput requirements of Virtual Reality (VR) applications must be above 400 Mbps to properly deliver a 4K VR 360° video experience [2] and even higher (above 1 Gbps) to provide an ideal (extreme) VR experience [3]. Technologies operating on it like Wi-Fi will be very important for those new applications because they consume a lot of spectrum resources [4]. Moreover, achieving those requirements is especially challenging in current dense scenarios with multiple Wi-Fi networks sharing the same channel, where the heightened contention and collision levels not only limit the achievable throughput but also impact the latency and reliability required by such stringent applications [5]–[7].

To address the challenges imposed by next-generation applications in high-density Wireless Local Area Network (WLAN) scenarios, the future IEEE 802.11bn amendment [8], [9] is likely to introduce Multi-Access Point Coordination (MAPC). This framework is envisioned to enhance the

overall latency and reliability performance, through alleviating channel access contentions in dense Wi-Fi deployments.

MAPC enables the introduction of different methods that perform coordinated resource allocation, such as Coordinated Time Division Multiple Access (C-TDMA), where Access Points (APs) agree on splitting time resources, or Coordinated Orthogonal Frequency-Division Multiple Access (C-OFDMA), where the agreement is on the allocated Resource Units (RUs) [8]. In certain scenarios, higher performance can also be achieved by enabling simultaneous transmissions through Coordinated Spatial Reuse (C-SR) and more complex techniques like Coordinated Beamforming (C-BF) or Joint Transmission (J-TX). Among these techniques, C-SR stands out as a particularly promising scheme since it can reduce latency and, in most scenarios, increase throughput, without requiring complex and resource-consuming measurement acquisition and coordination signaling [10]–[12]. For this reason, C-SR stands out as one strong candidate to be included in the next 802.11bn amendment.

The performance of MAPC techniques is still not fully understood. The definition of the MAPC framework started with IEEE 802.11be [13], but was then postponed until IEEE 802.11bn. Since then, multiple flavors of MAPC have been proposed, some advocating for decentralized solutions [14] and others for central controllers [15]. Another relevant point of discussion is related to the way coordination signaling should be performed, and whether over wireless or wired connections [14], [16]. Close in spirit to our work, [17] introduced a framework where compatible multi-AP groups are scheduled for performing simultaneous transmissions within a TDMA-slotted Transmission Opportunity (TXOP). The results in [17] evidenced that algorithms based on per-AP selection are preferable to those based on per-group selection.

When it comes to C-SR, its performance has been evaluated in a few IEEE 802.11 standard contributions [14], [18], [19] via simulation results, showing the potential gains compared with legacy access, C-TDMA, and C-OFDMA. In [20], the authors evaluated the throughput of networks implementing C-TDMA and C-TDMA with SR (C-TDMA/SR), showing that C-TDMA/SR leads to throughput gains between 50% and 140%, depending on the scenario, when compared to C-TDMA. As for the analytical characterization of C-SR,

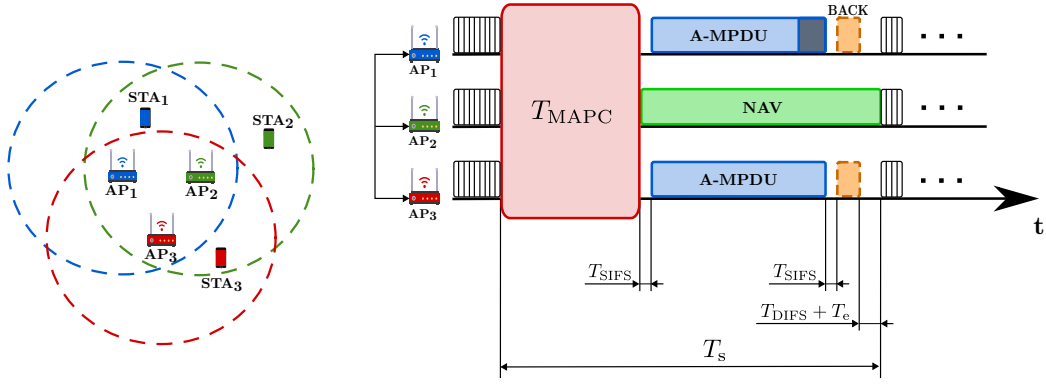


Figure 1. Left side: Example of the proposed MAPC operation in a small OBSS deployment. Right side: coordination frames and coordinated transmission, where AP₁ and AP₃ are selected due to their spatial reuse compatibility.

a model based on Markov chains was introduced in [21] to compute the C-SR's throughput and its spatial efficiency in comparison to the Distributed Coordination Function (DCF). However, the model in [21] did not consider backoff collisions and coordination overheads, which may affect the achievable performance gains. We aim to overcome such limitations.

Our contributions can be summarized as follows:

- We introduce a C-SR mechanism relying on the existence of spatial reuse groups of AP-Station (STA) pairs, i.e., groups of devices that can transmit simultaneously. Spatial reuse groups are periodically updated (e.g., every few hundred msecs) based on the exchanged Received Signal Strength Indicator (RSSI) reports between APs. Then, once the spatial reuse groups are updated, the data exchange phase starts, where TXOP sharing is used by the channel access winner to signal group transmissions.
- We leverage Bianchi's model to analyze the C-SR mechanism and evaluate its potential performance under full-buffer conditions. The presented analysis accommodates different group creation and selection algorithms, thus enabling to model and compare different implementations.
- Using the proposed analytical model, we evaluate the throughput of C-SR and compare it against DCF. Our results illustrate how the achievable throughput is affected by the devices' location. Moreover, they demonstrate the gains achieved by the proposed group formation approach, especially in scenarios with a large number of STAs per AP.

This paper focuses on throughput to evaluate the gains by leveraging C-SR capabilities compared to the traditional DCF in Wi-Fi networks. These gains can be turned into latency improvements and reliability, which is crucial for supporting applications with stringent performance requirements.

II. PROPOSED C-SR MECHANISM MODEL

A. C-SR Operation

We make the following modeling assumptions for the sake of tractability:

- We consider a group of APs within the same coverage area, i.e., Overlapping Basic Service Set (OBSS), that contend to access the channel using the default Carrier-Sense Multiple Access with Collision Avoidance (CSMA/CA) mechanism.
- The C-SR groups, i.e., the groups of AP-STA pairs that can benefit from SR concurrent transmissions, are computed based on the RSSI values exchanged between the coordinated APs. For low mobility scenarios, the RSSI varies on a slow time scale and its acquisition incurs limited overhead.
- The C-SR operation is implemented atop DCF in a TXOP-sharing fashion, i.e., when a coordinated AP gains access to the channel (i.e., the backoff counter reaches zero) it initiates a multi-AP transmission along with compatible transmitters in the OBSS. The AP that wins the contention (leader AP) then selects one of its STAs as a target receiver, and triggers the group (if exists) that includes other AP-STA pairs compatible with the target receiver.

The implementation of the overall coordination approach is illustrated in Fig. 1, where it can be seen how a set of coordinated APs compete to gain access to the channel using DCF. To capture the coordination overheads, we assume a coordination phase of duration T_{MAPC} . This phase includes channel reservation and information about the set of devices and settings to be used in the incoming coordinated TXOP, such as bandwidth, Modulation and Coding Scheme (MCS), TXOP duration, etc.¹ After the T_{MAPC} period, AP₁ and AP₃ start transmitting data in Aggregate MAC Protocol Data Units (A-MPDUs) to their corresponding STAs, while AP₂ sets its Network Allocation Vector (NAV), waiting its turn for decrementing its backoff. Subsequently, Block ACKs (BACK) are sent to AP₁ and AP₃ by their corresponding STAs using OFDMA.

¹We assume that the coordination phase is feasible and aligned with the MAPC mechanism being discussed and likely included as part of the IEEE 802.11bn amendment. However, details about its implementation are out of the scope of this paper.

B. Multi-AP Group Formation

An SR group consists of several APs and STAs pairs that are compatible, i.e., pairs of devices that can transmit simultaneously without causing the Signal-to-Interference-plus-Noise Ratio (SINR) at the served STAs to fall below a threshold γ_{CE} (see Section IV for further details). The groups are defined based on the RSSI perceived by each STA from the neighboring APs.²

Consider \mathcal{M} as the collection of all AP-STA pairs and \mathcal{C} as the ensemble of all valid combinations attainable (via exhaustive search) from the pairs within \mathcal{M} . Then, we define $\mathcal{M}_i \subseteq \mathcal{M}$ as the subset of the $M_i = |\mathcal{M}_i|$ active AP-STA pairs in the i -th combination, $i \in \mathcal{C}$. Moreover, the quality of each combination i is assessed by considering the total number of packets that can be transmitted by the M_i APs in combination i , i.e., $\rho_i = M_i \sum_{j \in \mathcal{M}_i} \varrho_{i,j}$, where $\varrho_{i,j}$ is the estimated number of packets correctly transmitted by AP-STA pair $j \in \mathcal{M}_i$, computed based on the MCS index employed by AP-STA pair j .

Using the computed combinations of feasible simultaneous transmissions, a subset $\mathcal{G} \subseteq \mathcal{C}$ is selected. Furthermore, to guarantee that all the AP-STA pairs are granted with a minimum number of transmission opportunities, we establish a constraint whereby a given AP-STA pair j can only be selected exactly φ times in \mathcal{G} , i.e., $\sum_{i \in \mathcal{G}} \mathbb{1}_{[j \in \mathcal{M}_i]} = \varphi$. For the sake of simplicity and without loss of generality, we set $\varphi = 1$ for the remainder of this paper, which means that an AP-STA pair j will only appear in a single group $i \in \mathcal{G}$.

To illustrate how the groups \mathcal{G} are selected, we consider the scenario in Fig. 2(a), where four BSSs (each formed by one AP and one STA) use the same channel. We assume that the RSSI measurements from all the AP-STA pairs in the scenario are available to every AP. Table I shows an excerpt of the combinations of AP-STA pairs and their associated score ρ_i . To choose among all possible groups, we sort them in descending order starting by the ones with the highest values of ρ_i . Moreover, the groups wherein one or more AP-STA pairs cannot decode frames properly due to the high interference generated are discarded, even if their associated ρ_i value is high. Following this mechanism, in the example shown in Table I, we would select combinations $\mathcal{G} = \{1, 4, 5\}$.

Table I
COMBINATIONS OBTAINED FOR DEPLOYMENT 1.

	AP ₁	AP ₂	AP ₃	AP ₄	ρ_i
1	STA ₁	-	-	STA ₄	1740
2	STA ₁	-	-	-	453
3	-	-	-	STA ₄	453
4	-	STA ₂	-	-	407
5	-	-	STA ₃	-	362

C. Group Transmission Probability

Every time an AP accesses the channel, i.e., its backoff counter reaches zero, it randomly selects one of its

²Owing to time division duplexing and channel reciprocity, downlink RSSI can be estimated from measurements on uplink frames (data or ACK frames).

STAs for transmission and, if the TXOP sharing is feasible based on the defined groups, it triggers the corresponding multi-AP group. Therefore, the probability that a group transmits is proportional to the number of AP-STA pairs that it contains. Thus, for group i , the transmission probability can be computed as:

$$\phi_i = \sum_{j \in \mathcal{M}_i} \alpha_j, \quad (1)$$

where α_j is the probability that AP-STA pair $j \in \mathcal{M}_i$, and therefore group i , is selected for transmission (i.e., STA j is selected for transmissions since its corresponding AP wins the channel contention). Following the full-buffer traffic assumption, and assuming that all the APs use the same access parameters and that STAs associated to each AP are selected with the same probability, we have that $\alpha_j = \frac{1}{KS_j}$, where K is the total number of APs in the network, and S_j the number of STAs associated to AP j .

For instance, the transmission probability of the groups selected in the example of Section II-B, i.e., $\mathcal{G} = \{1, 4, 5\}$, are calculated based on the probabilities that the involved STAs are served at a given TXOP. Therefore, the transmission probability of group 1, $\phi_1 = \frac{1}{4} + \frac{1}{4} = 1/2$ (notice that AP₁ and AP₄ only have one associated STA). Additionally, $\phi_4 = \phi_5 = 1/4$, because AP₂ and AP₃ transmit alone in their corresponding groups and have only one associated STA.

III. THROUGHPUT ANALYSIS

To investigate the attainable full-buffer throughput for C-SR, we extend Bianchi's DCF model [22] by introducing the concept of multiple AP transmissions enabled by C-SR within a single TXOP. Bianchi's DCF model applies to overlapping sets of devices and assumes a slotted time system, where the minimum slot unit corresponds to an empty slot ($T_e = 9\mu\text{s}$). The empty slot is also used as the unit for decreasing the backoff counter by one slot while contending for the channel. Apart from the empty slot, we find successful and collision slots. In the original Bianchi's model, a successful slot contains the transmission of only one device. However, in the context of C-SR, it can contain multiple simultaneous transmissions from the AP-STA pairs of a C-SR group. A collision slot, on the other hand, occurs when two or more devices finish their backoff countdown at the same time.

To compute the throughput of a given AP-STA pair j , we begin by calculating the probability of a device accessing the channel in a random slot time, given by:

$$\tau = \frac{1}{\mathbb{E}[B] + 1}, \quad (2)$$

where $\mathbb{E}[B]$ is the expected backoff in number of slots. Considering an infinite number of retransmissions per packet and utilizing the Binary Exponential Backoff (BEB) [23], we can compute $\mathbb{E}[B]$ as:

$$\mathbb{E}[B] = \frac{CW_{\min} + 1}{2} \left(\frac{1 - p - p(2p)^m}{1 - 2p} \right) - \frac{1}{2}, \quad (3)$$

where CW_{\min} denotes the minimum contention window, m is the number of backoff stages, and $p = 1 - (1 - \tau)^{K-1}$ represents the conditional collision probability. Since the conditional collision probability p depends on τ , and vice versa, both parameters need to be iteratively computed until convergence.

The average duration of a slot, $\mathbb{E}[T]$, can be expressed as:

$$\mathbb{E}[T] = p_e T_e + p_s \sum_{\forall i \in \mathcal{G}} \phi_i T_{s,i} + p_c T_c, \quad (4)$$

where, $p_e = (1 - \tau)^K$ and T_e are the probability and the duration of an empty slot given the coexistence of K transmitters, respectively, $p_s = K\tau(1 - \tau)^{K-1}$ represents the probability of a successful transmission slot, $T_{s,i}$ represents the duration of a transmission when group i is selected, and T_c is the duration of a collision slot. Besides, the probability that a slot includes a collision can be computed as $p_c = 1 - p_e - p_s$.

A successful transmission comprising group i has a duration of $T_{s,i}$, as it considers the maximum duration among all AP-STA pairs that transmit simultaneously in group i , i.e., $\max_{j \in \mathcal{M}_i} \{T_{i,j}\}$, and each of them depends on its own selected transmission rate, $R_{i,j}$. Thus the duration for AP-STA j can be computed as

$$T_{i,j} = T_{\text{MAPC}} + 2T_{\text{SIFS}} + T_{\text{DATA}}(R_{i,j}) + T_{\text{BACK}} + T_{\text{DIFS}} + T_e, \quad (5)$$

where all the signaling frames are transmitted using the basic rate.

Additionally, the aggregate throughput of the WLAN is

$$\Gamma = \frac{p_s L \left(\sum_{i \in \mathcal{G}} \phi_i \left(\sum_{j \in \mathcal{M}_i} N_{i,j} \right) \right)}{\mathbb{E}[T]}, \quad (6)$$

where L denotes the packet size, and $N_{i,j}$ is the A-MPDU size in number of packets that the STA in j receives from its corresponding AP for a transmission in group i . The term $\sum_{i \in \mathcal{G}} \phi_i \left(\sum_{j \in \mathcal{M}_i} N_{i,j} \right)$ represents the average number of packets transmitted in a successful slot, and it characterizes the throughput gain of C-SR compared to DCF. Notice that (6) holds for the particular case of DCF (without C-SR) if considering that each group contains a single AP-STA pair.

Finally, we can compute the throughput of AP-STA pair j by simply considering the number of transmitted packets by the target AP-STA pair in (6) instead of the entire group, i.e.,

$$\Gamma_j = \frac{p_s L \left(\sum_{i \in \mathcal{G}} \phi_i \left(\mathbb{I}_{[j \in \mathcal{M}_i]} N_{i,j} \right) \right)}{\mathbb{E}[T]}. \quad (7)$$

IV. PERFORMANCE EVALUATION

A. Scenario and System Model

We consider an OBSS with $K = 4$ full-buffered APs deployed throughout a squared scenario (see deployments in Fig. 2), with each AP separated by a minimum distance of $d_{\text{AP-AP}}$ meters from the others. The APs contend to access the same channel using DCF (they are assumed to

be within the communication range of the others), so packet collisions may occur during that process. Each AP k has S_k stations associated, which serves in a downlink manner. The STAs are randomly placed $d_{\text{AP-STA}}$ meters away from their corresponding AP. For the sake of simplicity, we consider the same number of STAs associated with each AP.

The transmission rate employed in a given AP-STA transmission depends on the MCS employed (we consider 802.11ax MCS values), which is selected based on the estimated RSSI at the receiver. As a result, stations close (far) from their AP are served using a higher (lower) MCS. The maximum number of aggregated packets in each A-MPDU depends on the MCS. We consider that all the APs use the same fixed transmit power. For an SR transmission to be successful, it is required that the SINR at the receiver surpasses a predefined capture effect threshold γ_{CE} [24]. Notice, as well, that this condition strongly depends on the set of concurrent AP-STA pairs selected for transmission in a TXOP.

The path loss effects $P_L(\text{dB})$ are modeled using the TGax model for Enterprise Scenarios [25]:

$$P_L = 40.05 + 20 \log_{10} \left(\frac{\min(d, B_p) f_c}{2.4} \right) + \mathbb{I}_{d > B_p} P' + 7W_n, \quad (8)$$

where d is the distance between the transmitter and the receiver in meters (but no less than 1), f_c is the carrier frequency in GHz, W_n is the number of walls traversed and P' is given by $P' = 35 \log_{10}(d/B_p)$.

We validate the results obtained with our analytical model using a simulator developed in Matlab reproducing IEEE 802.11 channel access in detail. Table II collects the parameters used in the evaluation. Note that we consider the same $T_{s,i}$ for all groups' transmissions, denoted by T_s , which results in different $N_{i,j}$ values for each STA and group.

B. Example Deployments

The two deployments presented in this section have been selected to illustrate how the performance of C-SR varies from one deployment to another, depending on the devices' location. Fig. 2(a) and Fig. 2(d) show the topology of Deployment 1 and Deployment 2, respectively. In both cases, we have $K = 4$ APs, the distance between access points is $d_{\text{AP-AP}} = 10$ meters, and a single STA per AP is randomly deployed $d_{\text{AP-STA}} \in [1, 10]$ meters away from it. Besides, Fig. 2(b) and Fig. 2(e) show the aggregate throughput (i.e., Γ) achieved under the DCF and C-SR schemes. Additionally, the bars drawn in Fig. 2(c) and Fig. 2(f) show the individual throughput experienced by each station in both deployments, when DCF and C-SR are applied. Black asterisks represent their corresponding throughput values obtained by simulation, showing a perfect match between analysis and simulations.

Deployment 1 is an example of a non-favorable deployment for C-SR, where only STA₁ and STA₄ can be served simultaneously, while STA₂ and STA₃ require to be served using alone transmissions. As indicated in Table I, the selected groups in this case are $\mathcal{G} = \{1, 4, 5\}$ (see

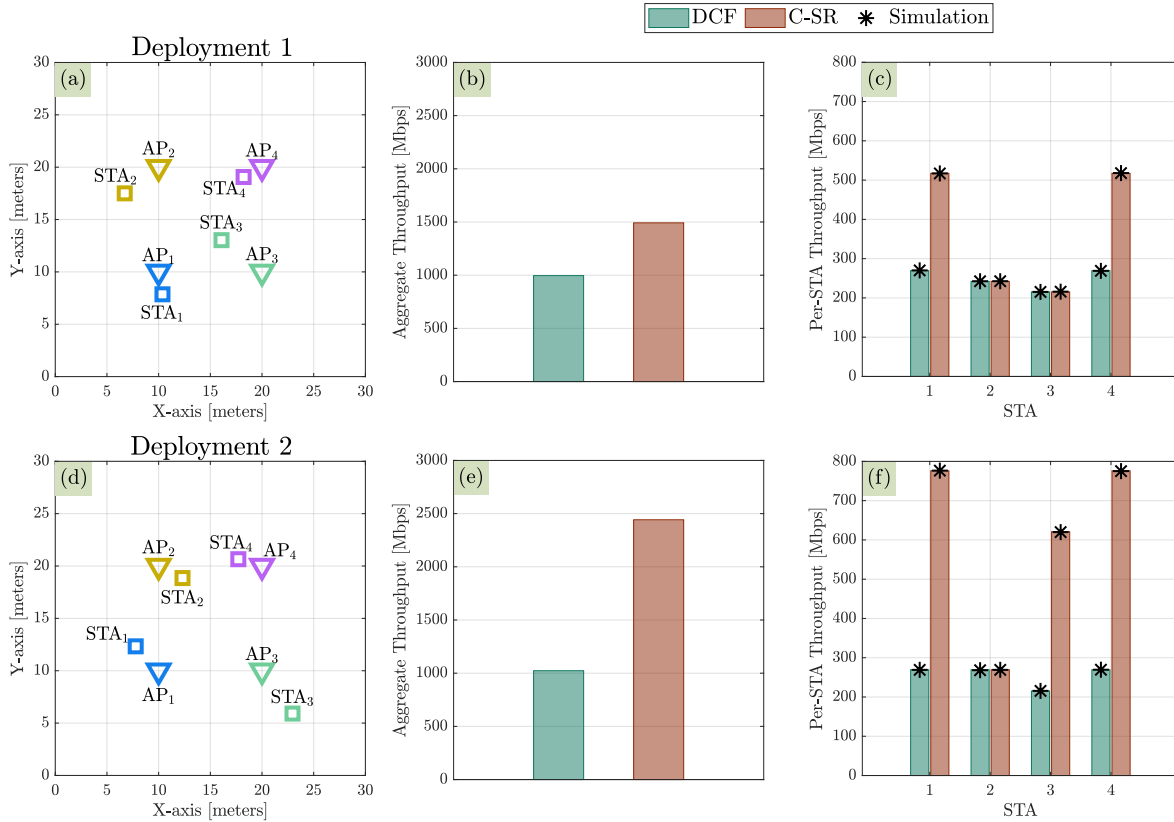


Figure 2. Deployment 1 and Deployment 2 are shown in (a) and (d), respectively. APs have been placed to a distance $d_{AP-AP} = 10$ meters, and 1 STA is associated to each of them. The aggregate throughput of DCF and C-SR in each deployment is shown in (b) and (e). Moreover, the throughput per STA in Deployment 1 and Deployment 2 are shown in (c) and (f), respectively.

Section II-B). The aggregate throughput in Fig. 2(b) shows a gain of 50% for C-SR with respect to DCF. This result is due to the higher number of gained TXOPs, and consequently, more transmissions by AP₁ and AP₄ because their group transmission probability is twice as high as the one of the APs that transmit alone, i.e., $\phi_1 = 1/2$ and $\phi_4 = \phi_5 = 1/4$.

On the other hand, the STAs in Deployment 2 in Fig. 2(d) are better located to form compatible C-SR groups. In this case, AP₁, AP₃, and AP₄ are selected to perform C-SR transmissions to their corresponding STAs, leaving only AP₂ alone, hence boosting the network's performance by around 139% with respect to DCF in Fig. 2(e). The per-STA throughput in Fig. 2(f) shows a remarkable gain exceeding 188% for C-SR with respect to DCF for all STAs except for STA₂, whose throughput is similar to the one under DCF since it is alone in its group.

C. Multiple Random Deployments

We also evaluate 1000 random deployment realizations for $d_{AP-AP} \in \{5, 10, 20\}$ meters, obtaining the throughput of each STA in all realizations. In each case, 10 STAs are deployed for each AP (for a total of 40 STAs) and placed $d_{AP-STA} \in [1, 10]$ meters from their corresponding AP. Fig. 3 illustrates the Cumulative Distribution Function (CDF) for DCF (continuous-black line) and C-SR (dashed-green, dotted-red, and light-blue lines, for 5, 10, and 20 meters, respectively). We observe that C-SR outperforms DCF in

all cases, achieving gains exceeding 73%, 188%, and 284% for the 95th percentile when $d_{AP-AP} = 5, 10$ and 20 meters, respectively. As expected, when d_{AP-AP} decreases, the interference generated by concurrent AP transmissions makes it unfeasible to exploit spatial reuse opportunities, with C-SR performing similarly to DCF in most scenarios. On the contrary, C-SR transmissions become more profitable when d_{AP-AP} increases, thus for $d_{AP-AP} = 10$ meters, only 1% of the groups contain 4 APs, while for $d_{AP-AP} = 20$ meters this proportion rises to 53%.

V. CONCLUSIONS

In this paper, we introduced a multi-AP coordination mechanism based on the formation of spatial reuse groups of AP-STA pairs, i.e., groups of devices that can transmit simultaneously. We leveraged Bianchi's model to analyze the C-SR mechanism and evaluate its potential performance under full-buffer conditions. Our study compared the throughput of C-SR against that of DCF and studied the trade-off between group size and interference depending on the locations of Wi-Fi devices. Our results highlighted the effectiveness of C-SR group formation and its potential for enhancing overall network performance, demonstrating a significant throughput improvement of up to 284% in certain cases. This approach could be further extended by including adaptive power control.

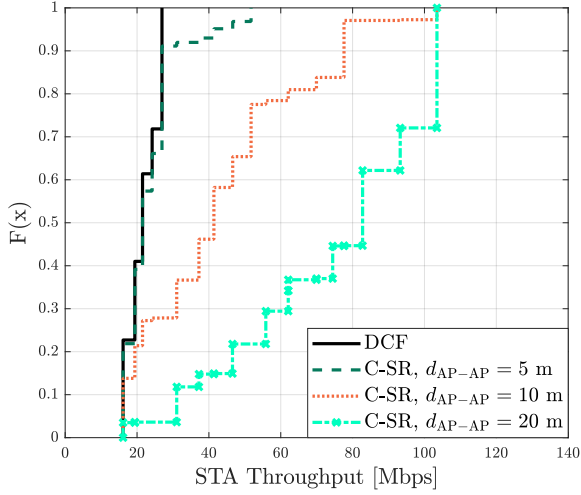


Figure 3. CDF of the STA throughput of DCF and C-SR, for $d_{AP-AP} = \{5, 10, 20\}$ meters and 10 STAs per AP.

Table II
SIMULATION PARAMETERS.

Parameter	Description	Value
d_{AP-AP}	Minimum distance between APs [meters]	$\{5, 10, 20\}$
d_{AP-STA}	Distance between AP and STAs [meters]	$[1, 10]$
B_p	Break-point distance [meters]	10
W_n	Number of walls (1 wall every 10 meters)	$\{0, 1, 2\}$
BW	Bandwidth [MHz]	80
f_c	Carrier frequency [GHz]	6
N_{SS}	Number of spatial streams	2
T_s	TXOP duration [ms]	5
T_c	Duration of a collision slot [μ s]	137
T_{MAPC}	Coordination overheads [μ s]	286
T_{BACK}	Block ACK [μ s]	100
CW_{min}	Min contention window	15
CW_{max}	Max contention window	1023
m	Number of backoff stages	6
T_e	Duration of an empty slot [μ s]	9
γ_{CE}	Capture effect threshold [dB]	15
EIRP	Effective Isotropic Radiated Power [dBm]	23
L	Length of single data frame [bytes]	1500

While we only presented a set of illustrative results due to space constraints, our analysis enables the evaluation of different group creation algorithms and TXOP sharing strategies. It also allows to study the effect of tuning key 802.11 parameters such as the allowed transmission rates, channel contention settings, and setting different transmission durations (e.g., per group).

VI. ACKNOWLEDGEMENTS

D. Nunez and B. Bellalta were supported by grant WiXR PID2021-123995NB-I00 (MCIU/AEI/FEDER,UE), by MCIN/AEI under the MdM Program (CEX2021-001195-M), and by SGR 00955-2021 AGAUR. G. Geraci was in part supported by the Spanish Research Agency through grants PID2021-123999OB-I00, CEX2021-001195-M, and CNS2023-145384, by the UPF-Fractus Chair, and by the Spanish Ministry of Economic Affairs and Digital Transformation and the European Union NextGenerationEU.

REFERENCES

- [1] D. Cavalcanti *et al.*, “Wireless TSN—definitions, use cases & standards roadmap,” *Avnu Alliance*, pp. 1–16, 2020.
- [2] S. Mangiante *et al.*, “VR is on the Edge: How to Deliver 360° Videos in Mobile Networks,” in *VR/AR Network '17: Proceedings of the Workshop on Virtual Reality and Augmented Reality Network*, 08 2017, pp. 30–35.
- [3] Wireless Broadband Alliance, “WBA Annual Industry Report 2023,” <https://wballiance.com/resource/wba-annual-industry-report-2023/>, October 2022, accessed on 11/05/2023.
- [4] E. Oughton *et al.*, “Reviewing wireless broadband technologies in the peak smartphone era: 6G versus Wi-Fi 7 and 8,” *Telecommunications Policy*, vol. 48, no. 6, p. 102766, 2024.
- [5] K. Meng *et al.*, “IEEE 802.11 Real Time Applications TIG report,” November 2018, doc.: IEEE 802.11-18/2009r6.
- [6] A. Aral *et al.*, “Addressing application latency requirements through edge scheduling,” *Journal of Grid Computing*, vol. 17, no. 4, pp. 677–698, 2019.
- [7] M. Carrascosa-Zamacois *et al.*, “Wi-Fi multi-link operation: An experimental study of latency and throughput,” *IEEE/ACM Transactions on Networking*, vol. 32, no. 1, pp. 308–322, 2024.
- [8] L. Galati-Giordano *et al.*, “What Will Wi-Fi 8 Be? A Primer on IEEE 802.11bn Ultra High Reliability,” *arXiv preprint arXiv:2303.10442*, 2023.
- [9] “IEEE 802.11-22/0078r3: 802.11 UHR Draft Proposed PAR,” <https://mentor.ieee.org/802.11/dcn/23/11-23-0078-03-0uhr-uhr-draft-proposed-par.docx>, January 2023, accessed on January 2024.
- [10] K. Aio *et al.*, “Overhead Analysis of Coordinated Spatial Reuse,” May 2023, doc.: IEEE 802.11-23/0616r0.
- [11] S. Helwa *et al.*, “Thoughts on Coordinated Spatial Reuse,” January 2024, doc.: IEEE 802.11-24/0120r0.
- [12] L. Lanante *et al.*, “Efficient Coordinated Spatial Reuse,” January 2024, doc.: IEEE 802.11-24/0095r0.
- [13] A. Garcia-Rodriguez *et al.*, “IEEE 802.11be: Wi-Fi 7 Strikes Back,” *IEEE Communications Magazine*, vol. 59, no. 4, pp. 102–108, 2021.
- [14] K. Aio *et al.*, “Coordinated Spatial Reuse Performance Analysis,” September 2019, doc.: IEEE 802.11-19/1534r5.
- [15] P. Nayak *et al.*, “Resource Management for Multi-AP Coordination,” April 2023, doc.: IEEE 802.11-23/0665r0.
- [16] T. Zeng *et al.*, “Multi-AP coordination over Fibre,” June 2023, doc.: IEEE 802.11-23/1186r1.
- [17] D. Nunez *et al.*, “Multi-AP Coordinated Spatial Reuse for Wi-Fi 8: Group Creation and Scheduling,” *arXiv preprint arXiv:2305.04846*, 2023.
- [18] D. Akhmetov *et al.*, “Multi-AP coordination for spatial reuse,” 2020, doc.: IEEE 802.11-20/0107r1.
- [19] Y. Seok *et al.*, “Coordinated Spatial Reuse (C-SR) Protocol,” April 2020, doc.: IEEE 802.11-20/0576r1.
- [20] D. Nunez *et al.*, “TXOP sharing with coordinated spatial reuse in multi-AP cooperative IEEE 802.11be WLANs,” in *2022 IEEE 19th Annual Consumer Communications Networking Conference (CCNC)*, 2022, pp. 864–870.
- [21] F. Wilhelmi *et al.*, “Throughput analysis of IEEE 802.11bn coordinated spatial reuse,” *arXiv preprint arXiv:2309.09169*, 2023.
- [22] G. Bianchi, “Performance analysis of the IEEE 802.11 distributed coordination function,” *IEEE Journal on Selected Areas in Communications*, vol. 18, no. 3, pp. 535–547, 2000.
- [23] B. Bellalta and K. Kosek-Szott, “AP-initiated multi-user transmissions in IEEE 802.11ax WLANs,” *Ad Hoc Networks*, vol. 85, pp. 145–159, 2019.
- [24] J. Lee *et al.*, “An experimental study on the capture effect in 802.11a networks,” in *Proc. ACM WiNTECH*, 2007, pp. 19–26.
- [25] S. Merlin *et al.*, “TGax Simulation Scenarios,” Nov. 2015, doc.: IEEE 802.11-14/0980r16.